Power and particle fluxes at the plasma edge of ITER : Specifications and Physics Basis

A. Loarte[1], M. Sugihara[1], M. Shimada[1]. A. Kukushkin[1], D. Campbell[1], M. Pick[1], C. Lowry[1], M. Merola[1], R.A. Pitts[1,2], V. Riccardo[3], G. Arnoux[3], W. Fundamenski[3], G.F. Matthews[3], S. Pinches[3], A. Kirk[3], E. Nardon[3], T. Eich[4], A. Herrmann[4], G. Pautasso[4], A. Kallenbach[4], G. Saibene[5], G. Federici[5], R. Sartori[5], G. Counsell[5], A. Portone[5], M. Cavinato[5], M. Lehnen[6], A. Huber[6], V. Philipps[6], D. Reiter[6], V. Kotov[6], R. Koslowski[6], G. Maddaluno[7], B. Lipschultz[8], D. Whyte[8], B. LaBombard[8], R. Granetz[8], A. Leonard[9], M. Fenstermacher[9], E. Hollman[9], P.C. Stangeby[9], M. Kobayashi[10], R. Albanese[11], G. Ambrosino[11], M.Ariola[11], G. de Tommasi[11], J. Gunn[12], M. Becoulet[12], L. Colas[12], M. Goniche[12], E. Faudot[13], D. Milanesio[14]

[1]*ITER Organization, CEA-Cadarache Centre, 13108 Saint Paul les Durance, France*
[2]*CRPP, Association EURATOM – Conféderation Suisse, 1015 Lausanne, Switzerland*
[3]*Euratom-UKAEA Fusion Association, Culham Science Centre, Abingdon OX113 3EA, United Kingdom*
[4]*Association Max-Planck Institut für Plasmaphysik, Boltzmannstr.2, D-85748 Garching bei München, Germany*
[5]*Fusion for Energy Joint Undertaking, C/ Josep Pla 2, 08019 Barcelona, Spain*
[6]*Association EURATOM - Forschungszentrum Jülich GmbH, D-52425 Jülich, Germany*
[7]*Association Euratom-ENEA Frascati, via Enrico Fermi 45, 00044 Frascati, Italy*
[8]*Plasma Science and Fusion Centre, MIT, 167 Albany Street, Cambridge, MA 02139, USA*
[9]*DIII-D National Fusion Facility, P.O. Box 85608, San Diego, CA 92186, USA*
[10]*National Institute of Fusion Science, 322-6 Oroshi, Toki 309-5292, Japan*
[11]*Consorzio CREATE, Via Claudio, 21, 80125 Napoli, Italy*
[12]*Association Euratom-CEA, CEA/DSM/DRFC, CEA Cadarache, F-13108 St. Paul-lez-Durance, France*
[13] *LPMIA, UMR 7040-C.N.R.S, Université de Nancy I, B.P. 239 54506 Vandoeuvre les Nancy, Francee*
[14]*Politecnico di Torino, Corso Duca degli Abruzzi 24, I-10129 Torino, Italy*

e-mail of main author : alberto.loarte@iter.org

Abstract. The physics basis for the evaluation of power fluxes on plasma facing components in ITER is described. The experimental and modelling basis for the specifications of these loads is summarised and the methodology followed for their extrapolation to ITER described.

1. Introduction.

As a result of the ITER design review activities, the specifications for power and particle fluxes onto plasma facing components (PFCs) have been revisited to incorporate the latest physics understanding of the processes leading to these loads and their scaling to ITER during both steady phases of the discharges and as a result of transients. Such specifications are required both for the detailed design of the PFCs as well as for estimating their lifetime when exposed to average and transient fluxes. It is particularly important to control transient fluxes in ITER (ELMs, etc.) to avoid temperature excursions which exceed material melting or sublimation points leading to erosion levels far above those expected in steady state. This paper summarises the experimental physics basis and the modelling/scaling methodology followed for the derivation of the magnitude of a selected set of these loads in ITER reference scenarios.

2. Power Fluxes to PFCs during steady phases of ITER discharges.

2.1. Power fluxes to PFCs during ramp-up/down phases.

The precise specifications in terms of plasma shaping (limiter versus divertor phases) and power/density requirements etc., of these phases is the object of on-going optimisation studies to take into account the various limits in the ITER coils, inductive flux requirements for Q_{DT}=10 operation, vertical stability etc., whose status is described in [1]. The present scenarios foresee initial and final ramp-up/down limiter phases in ohmic/low additional heating (P_{add}) L-mode conditions, while significant P_{add} may be applied during the diverted (L-mode and H-mode) phases. The results of the analysis of ohmic/L-mode edge power fluxes for divertor discharges from a multi-machine database [2] have been adopted for ITER. A

factor of ~ 2 around the predicted value for the power flux e-folding length (mapped to the outer midplane) has been assumed to account for uncertainties :

$$\lambda^{L}_{p}\,(m) = (1\pm1/3)\ 3.6\ 10^{-4}\ R(m)^{2}\ P_{div}(MW)^{-0.8}\ x\ q_{95}^{0.5}\ x\ n_{e}(10^{19}m^{-3})^{0.9}\ x\ Z_{eff}^{0.6} \qquad (1)$$

where R is the major radius of the device P_{div} is the conducted power to the divertor, n_e is the average plasma density and Z_{eff} is the plasma effective charge. During the ramp-up/down phases the plasma density is low compared to n_{GW} (Greenwald limit) [1] and the total level of radiation is therefore expected to be moderate (~30% of P_{input}) so that P_{div} ~ 0.7 P_{input}. Applying this scaling to derive λ_p for 15 MA L mode conditions near the H-mode transition (P_{input} = 40 MW, $<n_e>/n_{GW}$ = 0.4, Z_{eff} = 2.0) provides $\lambda_p^{L\text{-}15MA}$ = 1.0±0.3 cm. This is a factor of 2 larger than that expected for full performance Q_{DT} = 10 operation in H-mode [3], in reasonable agreement with the measured changes in λ_p at the H-mode transition. For H-mode conditions during the ramp-up/down phases it is, therefore, assumed that λ_p can be estimated on a similar basis from the L-mode scaling in (1), by dividing this calculated value by 2.

The same L-mode scaling has been applied to the limiter ramp-up/down phases in ITER by : a) replacing q_{95} by q_{LCFS} (which is about ~ 15% higher in limiter plasmas), b) replacing the power to the divertor by the power to the limiters and c) taking into account the effect of a variable number of poloidal limiters (i.e., the scaling in (1) corresponds to a large number of poloidal limiters) following the model in [4] for an arbitrary number N of (flat, i.e. a polygonal distribution) poloidal limiters. The highest power fluxes and narrowest λ_p derived from this methodology are similar to those obtained from EMC3-Eirene modelling of ITER edge plasmas based on experimental results from JET [5]. The spatial location of the limiter has been found to have an important effect on the measured λ_p in experiments. This is caused by edge transport in tokamaks having a strong ballooning component, which leads to larger λ_p when plasmas are limited on the high field side (HFS) [6, 7]. As a consequence, the local λ_p at the PFCs in contact with the plasma is expected to be ~ 4 times larger if the plasma is limited at the HFS than at the LFS (of this factor of ~ 4, 1.6 is due to the flux expansion at the HFS). This, together with the higher value of the toroidal field at the HFS yields expected local parallel power fluxes for a HFS limited phase in ITER which are similar to those predicted for a LFS limited phase ($q_{\parallel HFS}^{imp}/q_{\parallel LFS}^{omp}$ = 0.84).

The exact plasma conditions during these limiter phases are still the subject of on-going optimisation studies [1]. On the basis of present results [1] and for the purpose of defining the maximum power fluxes during limiter phases in ITER, the following prescription has been adopted P_{lim} (MW) < I_p (MA). This allows for some moderate level of additional heating (P_{add} = 3-5 MW) during the limiter phases for plasma currents I_p > 4 MA, in case it is required for optimising further these early/late phases of the discharges. As upper limits for the maximum I_p during ITER limiter phases the following values have been adopted : 5 MA (limiter-X-point transition for ramp-up) and 7.5 MA (X-point limiter transition for ramp-down). Scenario simulation studies in [1] show in fact that the ITER PF system actually permits these magnetic configuration transitions at much lower I_p.

An example of the parallel power fluxes onto the various PFCs in contact with the plasma during the ramp-up/down phases in ITER together with their outer midplane mapped decay lengths for typical L-mode conditions is shown in Fig. 1. For these results, the following assumptions have been made : **a)** the plasma density is maintained at $<n_e>/n_{GW}$ = 0.2, **b)** q_{95} ~ $3*(15/I_p(MA))^{0.7}$, which is approximately correct for the full-bore plasma ramp-up [1], **c)** Z_{eff} = $1.0+1.1/<n_e>(10^{19}m^{-3})$ (3.8 → 1.5 when I_p (MA) = 2.5 → 15), typical for ITER simulations [1] and consistent with a beryllium dominated plasma at the early stages of the discharge, **d)** $P_{lim,div.}$(MW) = 0.7 I_p (MA), which is typical for ohmic and low level of additional heating conditions and **e)** a range of outer to inner divertor power asymmetry $1 < P_{div,out}/P_{div,in} < 2$. Fig. 1 shows that even at these very moderate levels of P_{lim}, the parallel power fluxes for a plasma in the 2-port limiter configuration originally foreseen for ITER can reach very high values (close to ~ 100 MWm^{-2} for the conditions described above), as was originally shown in [5], which is challenging for their design (see [8]).

2.2. Power fluxes to PFCs during ITER Q_{DT} = 10 scenarios.

2.2.1. Power fluxes to the divertor during steady-state phases.

ITER is expected to explore a wide range of plasma conditions in divertor plasmas, which will cause a large range of plasma fluxes onto its PFCs. Since λ_p is usually found to decrease with I_p and P_{SOL} in H-modes [3], the largest power fluxes onto the divertor are expected to occur at the highest currents and powers. The methodology followed to determine λ_p for Q_{DT} = 10 conditions in ITER is based on two approaches : the first one is a direct scaling of the present experimental database [3, 9, 10]; the second is based on B2-Eirene modelling in conjunction with edge MHD stability modelling for ITER [11]. Both approaches provide the same estimate for Q_{DT} = 10 operation in ITER: λ_p = 5 mm.

The expected power fluxes at the ITER divertor for fully attached operation can be derived on the basis of B2-Eirene results [12] and extrapolation from present experiments. In fully attached conditions, the level of divertor radiation is low, typically ~ 20% of P_{SOL} (P_{SOL} = 80-100 MW for Q_{DT} = 10 in ITER) so that the power reaching the divertor is P_{div} < 80 MW. Assuming a range of outer to inner divertor power asymmetries 1 <$P_{div,out}/P_{div,in}$ < 2 leads to a maximum parallel power flux at either divertor target $q_{\|max}$ = 900 MWm^{-2}, corresponding to deposited power fluxes of up to ~ 40 MWm^{-2} [8]. It is important to note that divertor plasma conditions for these attached phases will almost certainly not be compatible with other requirements for the fusion performance of Q_{DT} = 10 operation (which in turn determines P_{SOL}), such as a sufficiently low level of core impurity, He exhaust etc. These attached conditions are therefore expected to occur only transiently when control of plasma detachment and divertor radiation fails (failure of plasma fuelling, impurity seeding, etc.) and are "naturally" limited in duration to periods whose length is determined by energy and particle confinement timescales in ITER (several seconds). Despite this relatively short duration, the associated power fluxes significantly exceed the power handling capability of the divertor target and, thus, such attached phases must be restricted to durations under ~ 1 s. This requirement (as well as minimising the possibility of such attached phases occurring at all) is being taken into account in the detailed design of the gas introduction system in ITER, which is the main actuator on the edge plasma density (DT gas fuelling) and divertor radiation (impurity seeding) allowing semi-detached operation to be recovered [13]. Apart from the need to restrict excessive transient heat loads, B2-Eirene modelling shows that for λ_p = 5 mm, the power handling requirements of the divertor target ($q_{div,peak}$ < 10 MWm^{-2}), He ash removal required for maintaining Q_{DT} =10 fusion performance etc., can only be achieved in conditions of high divertor radiation/semidetached divertor operation (typically P_{rad} ~ 70% of P_{SOL} by intrinsic or extrinsic impurities) [12]. The reduction by a factor of 4-6 of the peak divertor flux in semidetached conditions estimated by B2-Eirene with respect to the values for attached phases above is in good agreement with experimental observations in tokamaks (see for instance [14]).

2.2.2. Power fluxes to the main wall during steady-state phases.

Besides the divertor, the main wall of divertor tokamaks is subject to significant fluxes carried along the magnetic field by the plasma. These are in addition to other power fluxes such as those due to energetic atoms produced by charge-exchange and plasma radiation, which do not follow field lines. The origin of the parallel plasma fluxes is the turbulent nature of SOL transport, which leads to the fast radial convection of "blobs" in the far SOL of all tokamaks. The effective radial convective velocity in the outer SOL (v_{SOL}) of this transport is observed to increase with the distance from the separatrix in the SOL [15, 16] and with increasing separatrix plasma density and/or edge collisionality [16, 17]. Evaluation of the experimental database [15] indicates that v_{SOL} is weakly dependent on device size, as shown in Fig. 2 (from data in [16, 17, 18]). On the basis of this evaluation [15] and direct measurements of v_{SOL} from other devices [16], v_{SOL} = 30-100 ms^{-1} is predicted at the first field line intersecting the main wall in ITER. This corresponds to ΔR_{sep} = 0.05 m, which is the typical expected distance between the two plasma separatrices for high triangularity/near double-null plasma operation required for Q_{DT} = 10 operation. For the SOL field lines near

the inner wall, which are not magnetically connected to the outer SOL, the magnitude of the far SOL convective transport is much smaller than the values described above. This is due to the strong ballooning behaviour of transport in the SOL of both limiter and divertor plasmas. Measurements in present experiments operating in near double-null configurations [19] have been used to evaluate the magnitude of the far SOL convective transport in the inner wall disconnected SOL in ITER. On the basis of the SOL e-folding length measurements in [19], it expected that $v_{SOL}^{IN\text{-}SOL} = (1/3\text{-}1/5)\ v_{SOL}$, where $v_{SOL}^{IN\text{-}SOL}$ is the far SOL convective radial velocity in the disconnected SOL on the inner side.

While the magnitude of v_{SOL} directly correlates with the decay length of power fluxes in the far SOL region, the magnitude of the power flux itself at the near-far SOL interface is determined by near-SOL transport. The range of plasma parameters expected for ITER Q_{DT}=10 operation at this interface has been evaluated on the basis of results from B2-Eirene simulations [12] and direct empirical extrapolation of experimental data [9] : a) T_e = 20 eV, T_i/T_e = 2, $n_e = 5.0\text{x}10^{18}$ m^{-3} for low edge density conditions to b) T_e = 10 eV, T_i/T_e = 2, $n_e = 1.5\text{x}10^{19}$ m^{-3} for high density conditions. Taking into account that the transport in the far SOL is mainly convective allows the power decay length $\lambda_p = Lv_{SOL}/c_s$ to be evaluated (L ~ 60 m is the connection length of the field line covering a poloidal angle of π in ITER). The spatial profiles of the far SOL parallel power fluxes for a typical ITER Q_{DT}=10 equilibrium and plasma conditions (i.e. distance between separatrices ΔR_{sep} = 0.05 m and main separatrix-inner wall PFC distance of 0.15 m) are shown in Fig. 3. The maximum values for these fluxes are reached at the upper region of the device (near the second X-point), both because this is closest to the separatrix and because the toroidal field at this location is higher than at the outer midplane. The total power flux to the main wall associated with this far SOL transport in ITER is estimated to be $P_{far\text{-}SOL} < 20$ MW.

In addition to these steady-state fluxes, the main wall in ITER will be subject to energy and power fluxes associated with plasma radiation and charge-exchange neutrals. While the precise evaluation of these fluxes needs to be refined, their magnitude is not expected to exceed values of 0.25 MWm^{-2} for C-X atoms (including peaking by strong asymmetries in edge ionisation near the gas puffing system) and a similar value for plasma radiation. These loads reach the main wall PFCs in the direction orthogonal to their surface (on average). Similarly, extrapolation of measured loads by Marfes near the X-point [20] (which are unlikely to be compatible with the required plasma confinement for Q_{DT} = 10 operation) shows that the highest power flux in this event in ITER is ~ 1 MWm^{-2} and is deposited on the tungsten divertor baffles, for which the steady-state power handling capability is 5 MWm^{-2} [8].

2.2.3. Power/Energy fluxes on divertor and main wall PFCs by ELMs.

2.2.3.1. Divertor energy and power fluxes during ELMs.

Experimental evidence shows that the power flux to the divertor during ELMs is maximum near the separatrix, with a similar decay length at the divertor target to that measured between ELMs and has a high degree of toroidal symmetry [3]. Toroidally asymmetric structures can appear for field lines away from the separatrix at the divertor but power fluxes in these areas are typically more than one order of magnitude lower than for field lines close to the separatrix [21] and do not impose additional constraints for the design of the divertor target in ITER. On the basis of sheath transport scalings, the timescale for the rise phase of the ELM power deposition at the divertor target is expected to be in the range 250-500 μs for ITER [3]. The experimental time dependence of the ELM power deposition measured in JET and ASDEX Upgrade [22] is well reproduced by the model described in [23]. As a consequence, a significant amount of the ELM energy (typically more than 66%) is expected to arrive at the target after the maximum ELM power deposition on an expected timescale a factor of ~ 2 longer than the rise phase. Measurements of in/out ELM energy deposition asymmetries in JET and ASDEX Upgrade [24] show that for the favourable direction of the toroidal field for H-mode access, the ratio of inner to outer ELM energy

deposition is in the range of 1-2. The largest ELM loads in ITER are thus expected at the inner divertor. On this basis, the maximum energy density onto the inner and outer divertor targets can be estimated (with ~ 1.4 m^2 and ~ 1.9 m^2 the inner and outer effective areas for λ_p = 5 mm) :

$E_{in,div}^{max}$ (MJm^{-2}) $\leq 2/3*\Delta W_{ELM}(MJ)/1.4$ & $E_{out,div}^{max}$ (MJm^{-2}) $\leq 1/2*\Delta W_{ELM}(MJ)/1.9$ (2)

where $\Delta W_{ELM}(MJ)$ is the bulk plasma energy loss. The latter is predicted to be ~ 20 MJ for uncontrolled ELMs in ITER Q_{DT} = 10 conditions [25], corresponding to $E_{in,div}^{max}$ (MJm^{-2}) = 9.5, $E_{out,div}^{max}$ (MJm^{-2}) = 5.3 with an expected ELM frequency f_{ELM} = 1-2 Hz [25]. Experimental studies of PFCs (with specifications required for ITER) exposed to ELM-like transient loads have shown that significant erosion can occur if the surface temperature is such that sublimation (CFC) or melting (W) is approached [26]. This would reduce the divertor lifetime to few full performance discharges with uncontrolled ELMs in ITER [27]. This erosion threshold corresponds to energy densities in the range of 0.7-1.0 MJm^{-2}, while for energy densities of ~ 0.5 MJm^{-2} erosion is found to be negligible [26]. On this basis, requirements have been derived for ELM control in ITER consistent with negligible ELM erosion of the divertor targets resulting in a required maximum plasma energy loss for controlled ELMs in ITER of $\Delta W_{ELM}^{controlled} \leq 1$ MJ. The expected frequency for such controlled ELMs is $f_{ELM}^{controlled}$ = 20-40 Hz [25]. These requirements have been taken into account for the incorporation/detailed specification of ELM control strategy and schemes in ITER [28].

2.2.3.2. Main wall power and energy fluxes during ELMs.

Measurements of ELM energy deposition at the divertor and main wall in present experiments show that for conditions equivalent to those of uncontrolled ELMs in ITER, 5-20% of the ELM energy lost from the main plasma is deposited on main wall PFCs [29, 30]. The physics basis with which the details of the ELM power deposition on main wall PFCs in ITER can be predicted is still evolving. Estimates of the magnitude of ELM power fluxes must therefore account for insufficient knowledge in the key determining processes; for example: the formation, detachment and propagation of filaments during ELMs, the competition of the losses along the field line from the ELM filaments with their radial and toroidal propagation, etc.

In view of the incomplete understanding, a conservative approach has been followed to provide an upper estimate for the parallel fluxes to be expected during ELMs at the ITER first wall: **a)** the model in [23], which characterises the competition between parallel and radial energy transport during ELMs has been used to determine the expected values of the peak parallel power fluxes at the ITER main wall; **b)** it is assumed that the values of measured ELM radial propagation velocities do not scale with device size, a maximum value of v_{ELM} ~ 1 kms^{-1} for uncontrolled ELMs is used and it is assumed that this scales as $v_{ELM} \sim \Delta W_{ELM}^{1/2}$ for controlled ELMs (ITER fusion performance requires that pedestal parameters are not significantly affected by ELM control schemes); **c)** it is assumed, as a worse case scenario, that ELM plasma filaments detach from the separatrix radial position and that the plasma characteristics at the time of detachment are similar to those at the pedestal (namely $n_{ped} = 7.5\ 10^{19}\ m^{-3}$ and T_{ped} = 5 keV for ITER Q_{DT} = 10) [3] and **d)** it is assumed that the timescale for ELM power deposition by filament impact on the main wall is ~ 1/2 of that at the outer divertor, as seen in experiment and reproduced by modelling [21, 31]. These assumptions provide an upper limit for the maximum parallel energy flux deposited at the upper X-point region (ΔR_{sep} = 5cm) in ITER of :

$E_{\|,ELM}^{upper\text{-}X}$ = 1.0 MJm^{-2} (controlled ELMs) and 20 MJm^{-2} (uncontrolled ELMs), which when mapped to the outer midplane correspond to $E_{\|,ELM}^{mp}$ = 0.6 MJm^{-2} and & 12 MJm^{-2}, respectively. The range of decay lengths for the ELM energy deposition on the first wall is estimated to be λ_{ELM} = 0.025-0.09 m (mapped to the outer midplane). The typical estimated fraction of ΔW_{ELM} reaching the wall is under 10% for controlled ELMs and 20% or larger for uncontrolled ELMs. It is important to note that these maximum ELM parallel

energy fluxes on the first wall in ITER are one order of magnitude lower than the highest values at the separatrix itself (7.5 MJm^{-2} (controlled ELMs) and 150 MJm^{-2} (uncontrolled ELMs) at the outer midplane). This is in agreement with experimental measurements during uncontrolled ELMs in present experiments [21] and modelling predictions for ITER [31].

The assumptions above are reasonably conservative on the basis of present experimental evidence and understanding but it is important to note that these remain incomplete and are subject of intense research. For example, new experimental/theoretical results from experiments in which ELM energy losses are reduced by increasing pedestal collisionality (not a feasible strategy for achieving the requirements for controlled ELMs in ITER), indicate that v_{ELM} may scale with a weaker power of the normalised ELM energy loss : $v_{ELM}/c_{s,ped} \sim (\Delta W_{ELM}/W_{ped})^{1/4}$, if the spatial scale of the ELM filaments depends on $(\Delta W_{ELM}/W_{ped})$ [32]. Despite these uncertainties, predicted energy fluxes on ITER first wall based on direct extrapolation/modelling from results in present experiments (JET [32] and MAST [31]) with this prescription remain under the maximum values adopted for the ITER design following the approach described above. Fig. 4 shows the results obtained for the parallel ELM energy flux at the upper X-point region in ITER on the basis of the approach above and those derived from direct extrapolation from present experiments to ITER conditions (JET [32] and MAST [31]); the main difference between those being associated with the radial position of the filament at detachment (mid-pedestal point for JET extrapolations and separatrix for MAST extrapolations) and the normalisation of the MAST results to the separatrix ELM energy flux for controlled and uncontrolled ELMs foreseen for ITER.

In the absence of exposed edges in ITER main wall PFCs (which lead to close to normal incidence of field lines onto PFCs), the ELM energy fluxes to the main wall during controlled ELMs lead only to a relatively small additional power flux to the outer wall (ELMs fluxes are not observed in current devices to reach the inner wall for configurations close to DN, as in ITER) and should not cause any significant material erosion beyond that associated with physical sputtering of the impinging ions (i.e. no Be evaporation or melting for controlled ELMs). The absolute magnitude of the power arriving at the wall due to ELMs in ITER is expected to be small, typically less than 10% of the ELM power flux (P_{ELM} < 40 MW) i.e. 4 MW or 1/5 of the highest steady-state far-SOL transport power to the wall. However, contrary to the power fluxes in the far-SOL, main wall ELM fluxes are concentrated at the location of filament impact, which is expected to be random. The typical measured ratio of the filament FWHM to ELM filament separation is in the range 0.25-0.5 [32] so that a decrease of the ELM average power flux on the wall (compared to that which would be found if all ELM filaments would impact at the same static locations) by random impact in the range of 1.7-3.1 would be expected. For cases in which the ELM filament FWHM is approximately one half of the ELM filament separation, there is a significant probability that a series of ELM filaments will partially overlap at a wall location and the reduction of the power flux during this period will be smaller than the values given above. Evaluation of the number of events with significant ELM overlap and their duration has shown that this is limited to 0.5 s per discharge for controlled ELMs in ITER Q_{DT} = 10 conditions (10^4 ELMs per discharge), as shown in Fig.5.

From the evaluation of the energy parallel fluxes in ELM filaments above and their wall impact characteristics, the maximum parallel fluxes onto the first wall near the upper X-point for controlled ELMs with f_{ELM} = 20 – 40 Hz can be evaluated as:
$<q_{||,ELM}^{upper\text{-}X}>$= 12-24 MWm^{-2} with phases of $\Delta t < 0.5$ s in which $q_{||,ELM}^{upper\text{-}X}$ = 16-32 MWm^{-2}

The power fluxes at any location of the outer wall can be derived from these values by the using the appropriate value of the toroidal field at the point of consideration and the distance between that point and the separatrix mapped to the outer midplane.

2.3. Power fluxes to first wall and divertor during fast confinement transients.

Fast changes of the plasma energy in ITER can lead to the plasma separatrix approaching the first wall. This is due to the intrinsic time scale for the variation of the

currents in the external superconducting PF coils and the diffusion of the magnetic fields through the vacuum vessel (~ 1 s) which is comparable with the timescale of the transients. A typical example is a transition from full performance H-mode to L-mode caused by a sudden decrease of the power flux through the plasma edge, which could be caused by a failure of the additional heating, unexpected impurity influx, etc. It is important to note that for the ITER Q_{DT} =10 scenario $P_{SOL} < 2\ P_{L-H}$ and, thus, any significant decrease of edge power flux could trigger a H-L transition. To evaluate the maximum power fluxes to ITER PFCs during such transition, the following H-L transition scenario, based on results from divertor tokamaks, has been considered :

a) An initial phase with time duration of 30-200 ms during which the plasma pressure in the region r/a > 0.75 relaxes from H to L-mode causing an energy loss of $\Delta W_{L-H} < 60$ MJ [33].

b) A further decrease of the plasma energy to typical L-mode values (~ 130 MJ and P_{SOL} = 50 MW) within an L-mode energy confinement time of ~ 2 s.

c) The power flux e-folding length during this phase is $\lambda_p^{\ L} = 2\ \lambda_p^{\ H} = 1$cm.

As a result of such transition the plasma can shift radially inwards by ~ 10 cm or more [34] depending on the state of saturation of the central solenoid [1], causing significant power fluxes to reach the inner wall. This poses a major challenge for its design and calls for the development of mitigation strategies to avoid this plasma contact [8]. These fluxes have been evaluated in Fig. 6 for a range of assumptions with respect to the minimum distance between the separatrix and the inner wall in these events. Fig. 6 shows that contact of the plasma separatrix with the inner wall leads to parallel fluxes in excess of 250 MWm^{-2} for intervals that depend on the duration of this phase, which can last up to 3 s.

3. Conclusions.

The specifications of the power fluxes to the divertor and main wall during all phases of high performance scenarios in ITER have been derived on the basis of the most up to date physics understanding from experimental measurements and modelling. A similar evaluation has been carried out for loads associated with RF heating systems, VDEs and disruptive phases of these scenarios, but is not described in the paper due to space limitations. These specifications are being used to refine the detailed design of plasma facing components in ITER as well as of the systems required for their mitigation. Further refinement of these load specifications will be needed in areas where large uncertainties remain (for instance runaway loads) to incorporate the latest R&D results obtained at the ITER Members' fusion facilities/modelling groups.

Acknowledgement. This report was prepared as an account of work by or for the ITER Organization. The Members of the Organization are the People's Republic of China, the European Atomic Energy Community, the Republic of India, Japan, the Republic of Korea, the Russian Federation, and the United States of America. The views and opinions expressed herein do not necessarily reflect those of the Members or any agency thereof. Dissemination of the information in this paper is governed by the applicable terms of the ITER Joint Implementation Agreement.

4. References.

[1] Kessel, C., et al., IT2-3 this conference. [2] ITER Physics Basis, Nucl. Fusion **39** (1999) 2391. [3] Prog. on ITER Phys. Basis, Nucl. Fusion **47** (2007) S203. [4] Stangeby, P.C., et al., Proc 18th PSI Conference, 2008. [5] Kobayashi, M., et al., Nucl. Fusion **47** (2007) 61. [6] Harbour, P.J. and Loarte, A., Nucl. Fusion **35** (1995) 759. [7] Gunn, J., et al., J. Nucl. Mater. **363-365** (2007) 484. [8] Lowry, C., et al., IT1-4 this conference. [9] Kallenbach, A., et al., J. Nucl. Mater. **337-339** (2005) 381. [10] Whyte, D., et al., 9th ITPA Divertor and SOL Group, 2007. [11] Kukushkin, A., et al., Cont. Plasma Phys. **40** (2000) 233. [12] Kukushkin, A., et al., Nucl. Fusion **45** (2005) 608. [13] Pitts, R., et al., Memo on reattachment control (IDM reference ITER_D_2DMGEF) . [14] Loarte, A., et al., Nucl. Fusion **38** (1998) 331. [15] Lipschultz, B., et al., Nucl. Fusion **47** (2007) 1189. [16] Garcia, O., et al., Nucl. Fusion **47** (2007) 667. [17] Lipschultz, B., et al., Plas. Phys. Cont. Fusion **47** (2005). [18] Lipschultz, B., et al., Proc. 30th EPS Conf. Contr. Fus. Plas. Phys. (St. Petersburg, Russia, 2003). [19] LaBombard, B., et al., Nucl. Fusion **44** (2004) 1047. [20] Huber, A., et al., Proc 18th PSI Conference, 2008. [21] Eich, T., et al., Plas. Phys. Cont. Fusion **47** (2005) 815. [22] Eich, T., et al., Proc 18th PSI Conference, 2008. [23] Fundamenski,W.,et al., Plas.Phys.Cont.Fus. **48** (2006) 109. [24] Eich, T., et al., J. Nucl. Mater. **363-365** (2007) 989. [25] Loarte, A., et al., Plas. Phys. Cont. Fusion **43** (2003) 1549. [26] Klimov, N., et al., Proc 18th PSI Conference, 2008. [27] Federici, G., et al., Plas. Phys. Cont. Fus. **43** (2003) 1523. [28] Thomas, P., et al., IT1-5 this conference. [29] Herrmann, A., et al., Plas. Phys. Cont.

Fus. **46** (2004) 971. [30] Pitts, R., et al., Proc 18th PSI Conference, 2008. [31] Kirk, A., et al., Proc 18th PSI Conference, 2008. [32] Fundamenski, W., et al., EX4-3Ra this conference. [33] Loarte, A., et al., Memo on ITER loads specifications (IDM reference ITER_D_2ACXZB). [34] Portone, A., et al., IT/2-4Ra this conference.

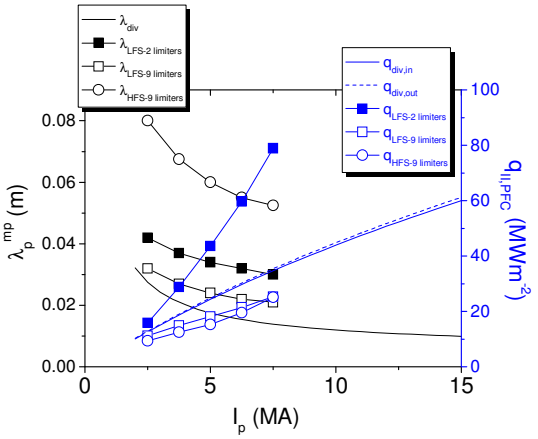

Figure 1. Calculated parallel power fluxes and power e-folding lengths mapped to the outer midplane at various PFCs in ITER (inner and outer divertor, 2 limiters at the Low Field Side, 9 Limiters at the Low Field Side and 9 limiters at the High Field side) for the L-mode assumptions described in the text

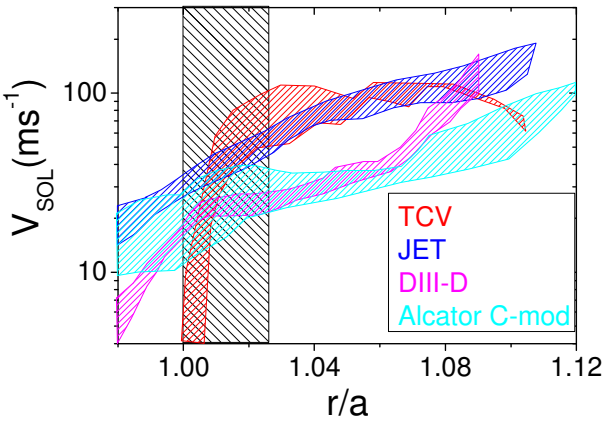

Figure 2. Derived effective plasma velocity in the SOL of various divertor tokamaks versus normalised distance to the separatrix (from [16, 17, 18]). The near SOL to far SOL division in this figure coincides with "standard" ITER operation near double null with a distance between the two separatrices ΔR_{sep} = 0.05 m

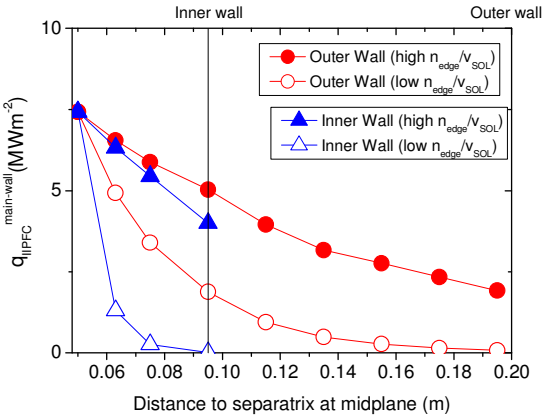

Figure 3. Calculated parallel power flux on the inner and outer wall for a range of assumptions concerning far-SOL transport for the ITER Q_{DT} = 10 scenario

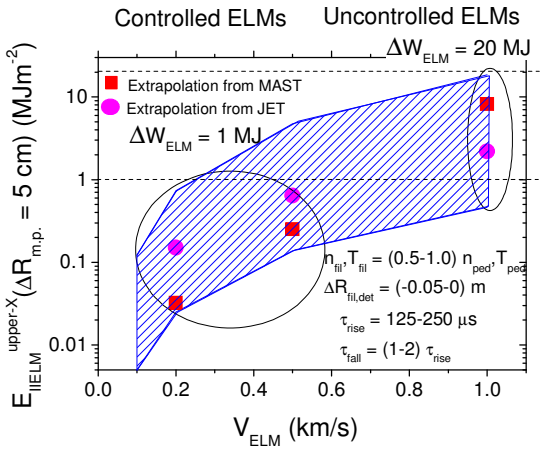

Figure 4. Calculated parallel energy fluxes during ELMs at the upper X-point region for the ITER Q_{DT} = 10 scenario for uncontrolled and controlled ELMs. The dashed area indicates the range for the ELM energy fluxes assumed for the ITER first wall design

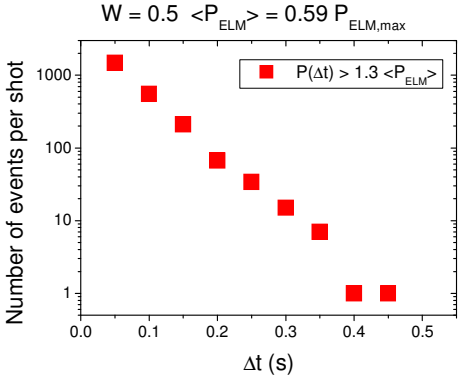

Figure 5. Number of events and associated time duration leading to significant ELM power fluxes above the average and their duration for FWHM-filament/ELM spacing = 0.5.

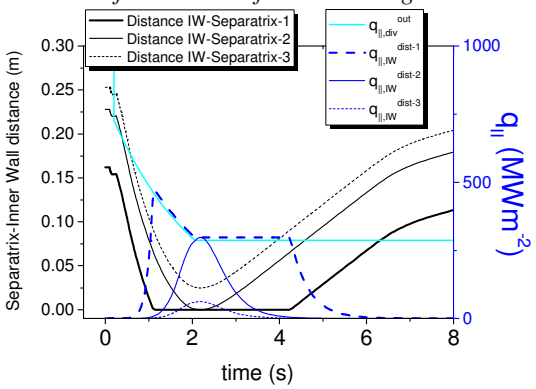

Figure 6. Parallel fluxes to the outer divertor target and inner wall following a fast L-H transition for a range of assumptions concerning the minimum distance between separatrix and inner wall during the transition